Historical trend of polycyclic aromatic hydrocarbons in a sediment core from Osaka Bay during the Meghalayan

Kai Nils Nitzsche[a, 1‡], Naoto F. Ishikawa[a], Toshihiro Yoshimura[a], Hiroto Kajita[a,b,c], Hodaka Kawahata[c,d], Nanako O. Ogawa[a], and Hisami Suga[a], Naohiko Ohkouchi[a]

[a] Biogeochemistry Research Center, Japan Agency for Marine-Earth Science and Technology (JAMSTEC), 2-15 Natsushima-cho, Yokosuka, Kanagawa 237-0061, Japan

[b] Graduate School of Science and Technology, Hirosaki University, 3, Bunkyo-cho, Hirosaki, Aomori 036-8561, Japan

[c] National Institute of Advanced Industrial Science and Technology, 1-1-1 Higashi, Tsukuba, Ibaraki 305-8567, Japan

[d] Atmosphere and Ocean Research Institute, The University of Tokyo, 5-1-5 Kashiwanoha, Kashiwa, Chiba 277-8564, Japan

Corresponding author:

‡ nitzsche@geo.tu-darmstadt.de, Tel.: +49-6151-1623687

Abstract

Polycyclic aromatic hydrocarbons (PAHs) are produced by incomplete combustion of biomass and fossil fuel, yet PAHs have been rarely analyzed in coastal sediment cores as a tracer for human activities before industrialization. The aim of this study was to assess if the historical trend of PAHs can be related to past human activities. To this end, we have

[1] Present address: Institute of Applied Geosciences, Technical University Darmstadt, Schnittspahnstraße 9, 64287 Darmstadt, Germany

determined the concentrations of PAHs in a 9 m-long sediment core from Osaka Bay, which records history of the last 2400 years. The concentration of PAHs before the beginning of the 17th century CE, the beginning of the peaceful Edo period, was consistently low (< 100 ng g^{-1}) and mainly comprised of smoke-derived PAHs reflecting the natural background. A relative higher abundance of 4−6 ring PAHs from the early 17th century CE and a higher PAH concentration from the early 18th century CE until approximately 1800 CE agreed with a population increase, Cu smelting activities and increasing combustion of charcoal. The constant PAH concentration until the late 19th century CE overlapped with a decline in the population in the Osaka area. An increasing PAH concentration from the late 19th century CE marked the beginning of industrialization in the Modern age. The peak in PAH concentration in 1945 CE was likely caused by burning of wooden structures due to air raids on Osaka City. A second peak around 1980 CE indicated the introduction of cleaner energies. We conclude that PAHs in coastal sediment cores can be used to reconstruct past human activities.

Keywords

Osaka Bay, sediment core, Meghalayan, polycyclic aromatic hydrocarbon, industrialization

Introduction

For millennia, humans have populated the land around estuaries due to the availability of freshwater, seafood, and fertile land (Allen, 2000; Lotze et al., 2006; Reeder-Myers et al., 2022). Estuaries are prone to accumulate pollutants from various natural and anthropogenic points and diffusive sources originating from their catchments (Barletta et al., 2019; de Souza Machado et al., 2016; Islam and Tanaka, 2004). Sediment cores from coastal areas are valuable archives for reconstructing past climate conditions including sea-surface temperatures (SST), ancient population changes and shifts in social systems (e.g., Kajita et al., 2018, 2023; Kawahata et al., 2017) and early agricultural and smelting activities (Sun et al., 2016; Zong et al., 2010). Furthermore, polycyclic aromatic hydrocarbons (PAHs), a proxy for climate-driven or human-related historical fires and biomass and charcoal burning, accumulate in coastal sediment cores.

Humans have burnt biomass and charcoal for millennia through domestic fires, forest clearings, stubble burning, and fueling manufactures such as smelting. More contemporaneous activities are the burning coal, oil, gas for industrial activities and the combustion of gasoline in vehicular traffic. Furthermore, natural wildfires are common around the globe. PAHs are formed as a natural byproduct of incomplete combustion of biomass and carbonaceous fuels (Wilcke, 2007). The carbon and hydrogen content of PAHs partly reflect their source. Diagnostic ratios can be used to distinguish between petroleum, biomass, and coal (Tobiszewski and Namieśnik, 2012; Yunker et al., 2002), which allow us to distinguish plant communities (gymnosperms vs. angiosperms) or smoke and combustion residues (Karp et al., 2020). PAHs enter the marine environment via atmospheric deposition, or directly via oil spills, ship traffic, and river discharge (Baek et al., 1991; Wang et al., 1999; Yunker et al., 2002). PAHs are eventually deposited in the sediment. Owing to their low biodegradability due to the lack of functional groups, the historical trend of PAHs is well preserved in sediment cores from freshwater lakes and ponds. Therefore, PAHs can be related

to past human activities such as forest fires, biomass and fossil fuel burning (Argiriadis et al., 2018; Elmquist et al., 2007; Slater et al., 2013; Topness et al., 2023; Vachula et al., 2022; Yan et al., 2005). Furthermore, several studies have discussed the temporal variation in PAHs in coastal sediment cores with reference to industrial and traffic-related emissions (Guo et al., 2023; Kuo et al., 2011; Lazzari et al., 2019; Liu et al., 2005; Yamashita et al., 2000; Yan et al., 2006; Yoon et al., 2023). It is expected that the PAH record in coastal sediments cores also indicates pre-industrial human activities such as biomass and charcoal burning especially during ancient times.

Osaka Bay is located directly next to Osaka City, which is part of the Kyoto-Osaka-Kobe metropolitan area, the second most urbanized area in Japan. Osaka City has experienced industrialization and urbanization since the 1890s CE and has emitted a large amount of trace metals during the post-World War II economic growth period in Japan (Hosono et al., 2010; Nitzsche et al., 2022; Yasuhara and Yamazaki, 2005). Tsuji et al. (2020) found that PAH concentrations in a young (< 50 years) sediment core from Osaka Bay peaked around 1980 CE and declined since then until now. Ishitake et al. (2007) and Moriwaki et al. (2005) suggested that the burning of wooden structures followed by the intense bombing of Osaka City led to a peak in PAHs around 1945 in a sediment core from Nagaike Pond and from Osaka Castle moat, respectively. Moriwaki et al. (2005) also noted that increasing PAHs concentrations in pre-industrial times (1680 to 1880 CE) were attributed to wood burning by humans. Yet, such small catchments could be impacted by nearby events like fires. Information on the historical trend of PAHs is present in the 17th century CE. Osaka, formerly known as Naniwa, has a long history dating back to the Kofun period (250 to 592 CE), was scenery of repeated warfare during the Sengoku period (1467 to 1615 CE), experienced an increase in the population and metal smelting activities and became an important economic hub during the Edo period (1603 to 1867 CE) (Table 1). Thus, early

human activities such as wood and charcoal burning for domestic fires and smelting could have led to high PAH emissions.

In this study, we investigated the temporal variation in PAH concentrations and diagnostic ratios in a 9 m-long sediment core from Osaka Bay, which records a history of the last 2,400 years. The aim of this study was to assess if the historical trend of PAHs can be related to past human activities. In our previous study, we found increasing trace metal concentrations in the core from the early 17th century CE due to early human activities (Nitzsche et al., 2022). Thus, our second goal was to compare the PAH concentration to trace metal concentrations in order to identify similar trends and sources.

Study area and sampling

Osaka Bay and its catchment

The catchment of Osaka Bay is located in Central Japan and covers a total area of approximately 10,700 km^2 with the Yodo River catchment being the largest (8,240 km^2). Coniferous forests dominate the catchment of Osaka Bay; yet large urban and build-up land areas are present owing to the Kyoto-Osaka-Kobe (Keihanshin) metropolitan area. Lake Biwa is located in the northeastern part of the catchment with an area of approximately 3,170 km^2. The geology of the whole catchment consists mainly of Quaternary unconsolidated sediments (Itihara et al., 1988), clastic (meta)sedimentary rocks of the Jurassic and Cretaceous accretionary complexes, Cretaceous granitoid rocks, felsic volcanic and volcanoclastic rocks, and minor gneisses and schists, Carboniferous to Permian limestones and basalts, and Cretaceous gabbro.

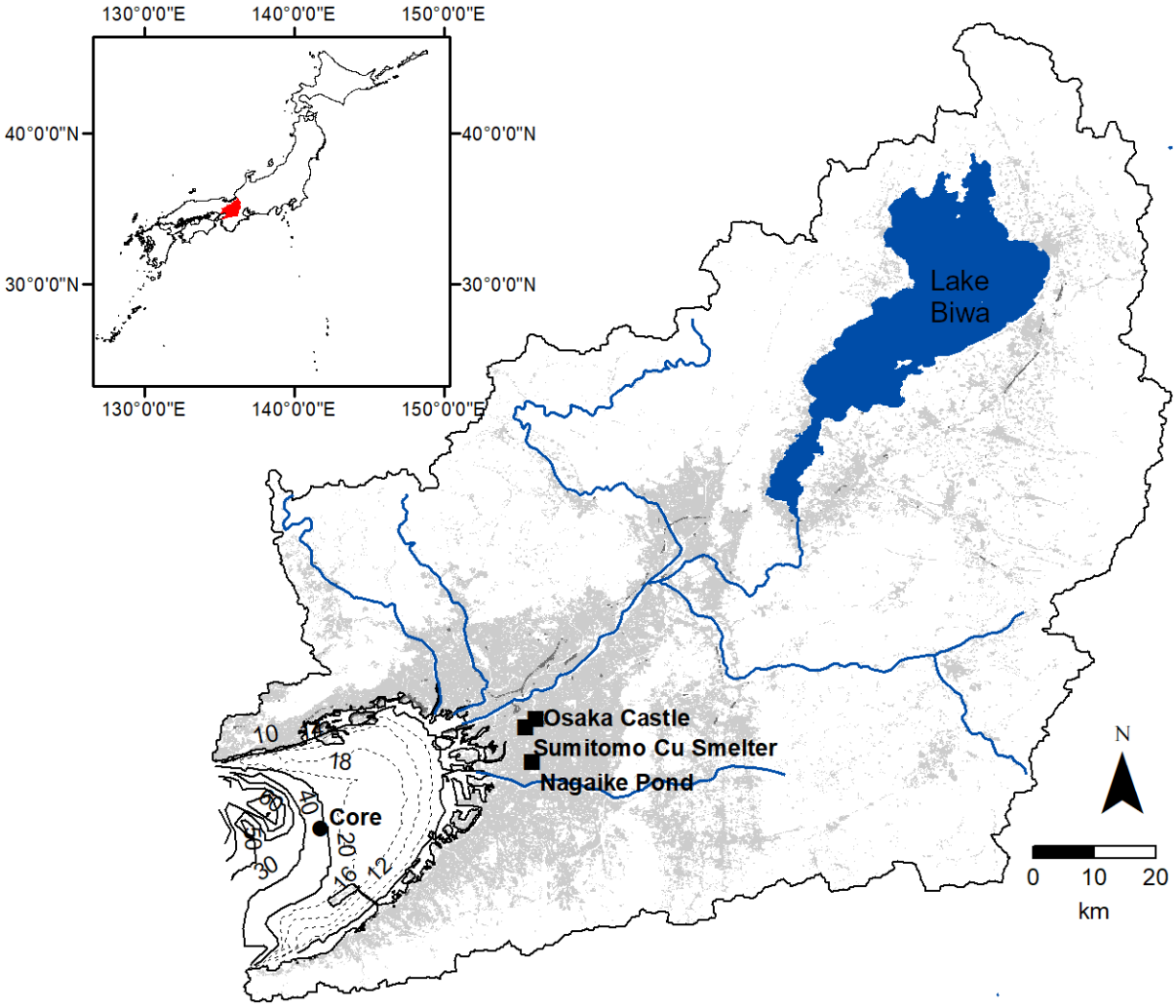

Figure 1. Location of the Osaka Bay catchment in Japan (top left), and area of urban land in grey with major rivers and the locations of the sediment core, Osaka Castle, the Sumitomo Cu smelter and Nagaike Pond (bottom right). Note that Osaka Castle was constructed on the grounds of the former Ishiyama Hongan-ji temple. The former site of Naniwa-no-Miya Palace was directly adjacent to the later built Osaka Castle. Land-use data were obtained from Land Use Fragmented Mesh Version 2.5.1 from the National Land Numerical Information, created by Ministry of Land, Infrastructure, Transport and Tourism, the Government of Japan.

Sediment sampling

A piston core was collected at station OS5B from the central part of Osaka Bay at a water depth of 24 m during cruise KT-11-13 on July 1, 2011 (Fig. 1). The core was cut in 2

127 cm-slices from the surface to the final core depth of 884 cm (see for further details Nitzsche et
128 al., 2022).
129
130 *Historical events in the catchment*
131 Since the early Holocene, about 7000 BCE, Osaka Bay and its catchment underwent
132 many natural (Kajiyama and Itihara, 1972; Matsuda, 2008; Yasuhara et al., 2002) and
133 artificial transformations (Pearson, 2016) as well as other human activities, which affected the
134 sedimentation rates and sediment sources, and probably the PAH input into the bay. In
135 particular, the brackish Kawachi Lagoon was transformed into Kawachi Lake during 400
136 BCE to around 1 BCE, into the marshland Kawachi Plain from around 800 CE, and finally
137 into the present Osaka plain from the second half of the 19th century CE (Kajiyama and
138 Itihara, 1972; Matsuda, 2008). Permanent habitation on the Uemachi Plateau and around the
139 Kawachi Plain started as early as 700 BCE (Pearson, 2016). The major events have been
140 reported in our previous work (Nitzsche et al., 2022), however, they are summarized in the
141 current study (Table 1), and the situation during the 3rd and 4th centuries CE is shown in
142 Figure S1.

143 Table 1. Historical events in Osaka (Naniwa) City and the Osaka Bay catchment.

Period	Year	Event
Modern (1868 CE to present)	1960s CE	Transition from coal to oil
	1945 CE	Air raids destroyed large areas
	1940-1945 CE	WWII
	1929-1932 CE	Economic recession
	1914-1918 CE	WWI
	1904/1905 CE	Russo-Japanese War
	1894/1895 CE	First Sino-Japanese War
	1890s CE	Start of industrialization
	1868 CE	Opening of the port for trade
Feudal (1185 to 1868 CE)	1863 CE	Big city fire
	1837 CE	Big city fire
	1724 CE	Big city fire
	1690 CE	Expansion of the Sumitomo Copper Refinery
	1620s CE	Reconstruction of Osaka Castle
	1614/1615 CE	Siege of Osaka Castle
	1583 CE	Construction of Osaka Castle
	1569-1580 CE	Siege on Ishiyama Hongan-ji temple
	1492 CE	Completion of Ishiyama Hongan-ji temple
Imperial and aristocracy (592 to 1185 CE)	1180 CE	Completion of the Fukuhara Palace
	726 CE	Completion of Naniwa-no-Miya Palace
	686 CE	Naniwa Nagara-Toyosaki Palace burned down
	652 CE	Completion of Naniwa Nagara-Toyosaki Palace
	593 CE	Completion of Shitenno-ji temple
Transition (Kofun) (250 to 592 CE)	5th century CE	Digging of the canal Naniwa no Horie Construction of the port facility Naniwa-tsu Start of iron smelting (*tatara*)
Yayoi (930 BCE to 250 CE)	From 700 BCE	Rice cultivation and permanent habitation

144

Material and methods

Core dating

The dating of the core has been previously described (Nitzsche et al., 2022). Briefly, the piston core has been dated by 22 radiocarbon measurements of molluscan shells using accelerator mass spectrometry (AMS) at the Micro Analysis Laboratory of the University of Tokyo (Matsuzaki et al., 2004; Yokoyama et al., 2019). The technique employed for sample preparation was previously reported (Yokoyama et al., 2007). The radiocarbon age results were calibrated to calendar years using the OxCal ver. 4.4 software (Bronk Ramsey, 2009) with the Marine 20 dataset (Heaton et al., 2020) assuming a regional specific reservoir (DR) correction of 135 ± 20 years (Kuwae et al., 2013), which was estimated for Beppu Bay, located in the Seto Inland Sea which is about 350 km west from our study site. The core provided a continuous environmental record of the last 2,300 years (Fig. 2).

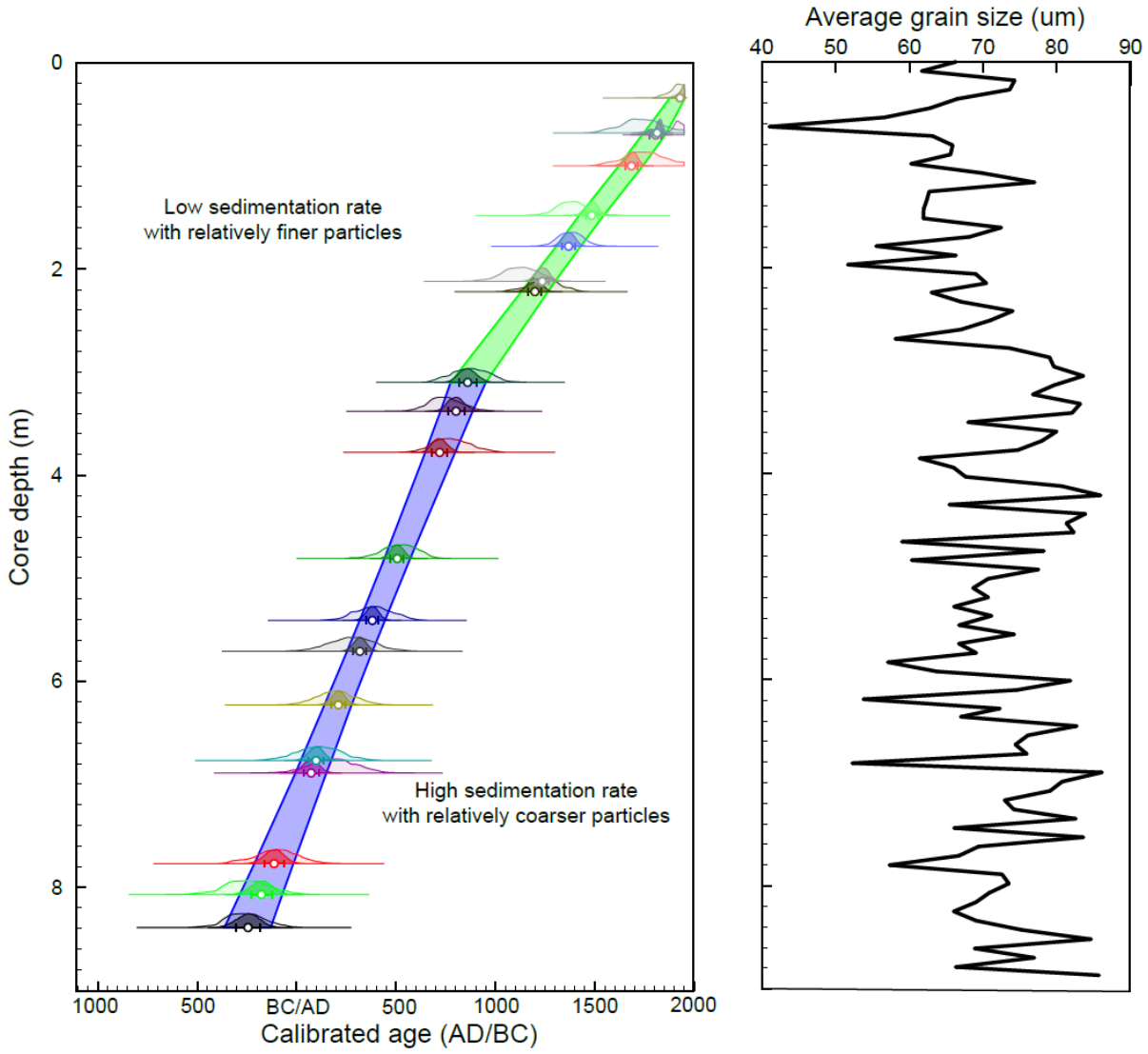

Figure 2. Core depth (cm) versus calibrated age of the piston core (a). For each ^{14}C age controlling point, P-sequence modeled and unmodeled age probability distributions are shown. The error bars represent the 1σ error of the P-sequence modeled age. Average grain size (b). Figure reproduced from Nitzsche et al. (2022).

Core logging

The sedimentary facies comprised of a homogenous olive grey mud inferred by X-ray computed tomography (CT) measurement at Kochi Core Center, JAMSTEC. The wet density of the core was determined via gamma ray transmission using a Multi-Sensor Core Logger (Geotek Ltd., Daventry, UK) at Kochi Core Center.

Total organic carbon concentration and stable isotope analysis

The total organic carbon (TOC) and carbon stable isotope ratios ($\delta^{13}C$) were determined for 61 sediment samples from selected horizons after freeze-drying, sieving to < 125 μm, and manually powdering. TOC concentrations and $\delta^{13}C$ values were determined after weighing samples into pre-cleaned smoothed wall tin capsules, decalcification with 0.5M HCl and drying on a hotplate at 80 °C. The tin capsules with the dried samples were sealed, and analyzed using a sensitivity-improved elemental analyzer (Flash EA1112, Thermo Finnigan, Bremen, Germany) connected to an isotope ratio spectrometer (Delta plus XP, Thermo Finnigan, Bremen, Germany) at the Biogeochemistry Research Center (BGC), JAMSTEC, according to Ogawa et al. (2010). The isotopic values are expressed in delta notation (‰), relative to VPDB (Vienna Pee Dee Belemnite) standard. The carbon isotopic compositions were calibrated using five inter-laboratory determined standards, which ranged from -26.86 ‰ to 0.18 ‰ (BG-T: L-tyrosine, BG-A: L-alanine, BG-P: L-proline, Tayasu et al., 2011; L-Valine and L-Glutamic acid, Sun et al., 2023, Shoko Science Co., Ltd.). Analytical errors of the $\delta^{13}C$ values estimated with repeated analyses of BG-T was ±0.20 ‰ (1σ; n =14).

Extraction and analysis of polycyclic aromatic hydrocarbons

Fifty-six samples were selected for PAH analysis to have one or two samples during each century before the 17th century CE, and every 10 to 20 years after the 17th century CE. The lipids of the samples (1.0 or 2.0 g) were extracted twice for 15 min by sonication using a mixed solvent of dichloromethane/methanol (70:30, v/v). The extracts were evaporated, re-dissolved in hexane, and loaded on deactivated 1 % H_2O silica gel columns pre-conditioned with hexane. The N-1 fraction (hydrocarbons) was extracted with *n*-hexane, and the N-2 fraction (ketone, aldehyde, eater) with *n*-hexane/dichloromethane (50:50, v/v). Subsequently, the N-1 and N-2 fractions were analyzed for PAHs using gas chromatograph-mass

spectrometry (GC-MS) (Agilent 7890A-GC with Agilent 5975C inert XL MSD) equipped with the VF-5ms column (0.25 mm ×30 m, film thickness 0.10 μm) at the BGC. The oven temperature was programmed as follows: maintained at 40 °C for 2 min, raised up to 120 °C at 30 °C min^{-1}, then to 320 °C at 6 °C min^{-1}, and maintained at 320 °C for 20 min. Helium was used as the carrier gas with a constant flow are of 1 mL min^{-1}. A standard containing naphthalene (Nap), acenaphthylene (Acy), acenaphthene (Ace), fluorene (Flu), phenanthrene (Phe), anthracene (Ant), fluoranthene (Flt), pyrene (Pyr), benz[a]anthracene (BaA), chrysene (Chr), benzo[b]fluoranthene (BbF), benzo[k]fluoranthene (BkF), benzo[a]pyrene (BaP), indeno[1,2,3-cd]pyrene (IcdP), dibenz[a,h]anthracene (DahA) and benzo[g,h,i]perylene (BghiP)) (AccuStandard, USA) was prepared and analyzed together with the samples for identification and quantification of PAHs (Table 2). Additionally, a perylene standard was analyzed. Peak areas of individual PAHs were obtained in selected ion monitoring (SIM) mode and used for the quantification. The concentration of PAHs in three analytical blanks were below the detection limit. To account for any losses of individual PAHs during the sample preparation, a PAH standard was evaporated and treated as the samples. The recovery rates ranged from 70 to 90 % for 3-ring PAHs, from 90 to 100 % for 4-ring PAHs, and were around 100 % for 5- and 6-ring PAHs.

We calculated the ratio of Flt/(Flt+Pyr) as a proxy for PAH sources, i.e., a ratio Flt/(Flt+Pyr) smaller than 0.4 indicates petroleum leakage, between 0.4 to 0.5 is indicative of petroleum combustion, and larger 0.5 is characteristic of biomass and coal combustion (Yunker et al., 2002). A IcdP/(IcdP+BghiP) ratio of below 0.2 is indicative of petroleum, between 0.2 and 0.5 of petroleum combustion, and greater than 0.5 of biomass and coal combustion (Yunker et al., 2002). Furthermore, we calculated the ratio of the low molecular weight PAHs Phe + Ant +Flt + Pyr (LMW) relative to the sum of PAHs (LMW/total). Smoke-derived PAHs have a LMW/total ratio between 0.75 and 0.9, and combustion residues have between 0.3 and 0.8, respectively (Karp et al., 2020). We also compared the total

concentration of PAH (ΣPAH) with metal concentrations in the same sediment core that were reported in our previous paper (Nitzsche et al., 2022) to estimate PAH sources.

Table 2. List of the 17 polycyclic aromatic hydrocarbons (PAH) analyzed in this study, with their number of rings and molecular weight.

Compound	Abbreviation	Rings	Molecular weight (g mol^{-1})
Naphthalene	Nap	2	128
Acenaphthylene	Acy	3	152
Acenaphthene	Ace	3	154
Fluorene	Flu	3	166
Phenanthrene	Phe	3	178
Anthracene	Ant	3	178
Fluoranthene	Flt	4	202
Pyrene	Pyr	4	202
Benz[a]anthracene	BaA	4	228
Chrysene	Chr	4	228
Benzo[b]fluoranthene	BbF	5	252
Benzo[k]fluoranthene	BkF	5	252
Benzo[a]pyrene	BaP	5	252
Perylene*	Per	5	252
Benzo[g,h,i]perylene	BghiP	6	278
Dibenz[a,h]anthracene	DahA	5	278
Indeno[1,2,3-cd]pyrene	IcdP	6	276

* Not included in the sum of total PAHs

Results

Density, carbon stable isotopes and total organic carbon

The wet density was relatively constant and usually ranged from 1.3 to 1.7 g cm^{-3} (Fig. S2). The $\delta^{13}C$ values varied from –22.7 ‰ to –21.0 ‰ except for an outlier (−24.5 ‰) around the beginning of the Heian period at approximately 850 CE (Fig. 3). The TOC content varied between 0.83 % and 1.02 % from around 320 BCE to 1870 CE. Since then, the TOC content continuously increased to 1.51 % at the surface.

We found that the only little variations in the wet density, the $\delta^{13}C$ values and TOC %, the homogenous olive grey mud, the relatively constant grain size distribution, and the

236 constant sediment accretion rate (SAR) except for a drop around 800 CE (Fig. 2) (Nitzsche et
237 al., 2022), suggesting that the grain density and porosity do not drastically change throughout
238 the core. Therefore, we suggest an almost constant mass accumulation rate (MAR) and that
239 the PAH concentrations are roughly parallel with the MAR.

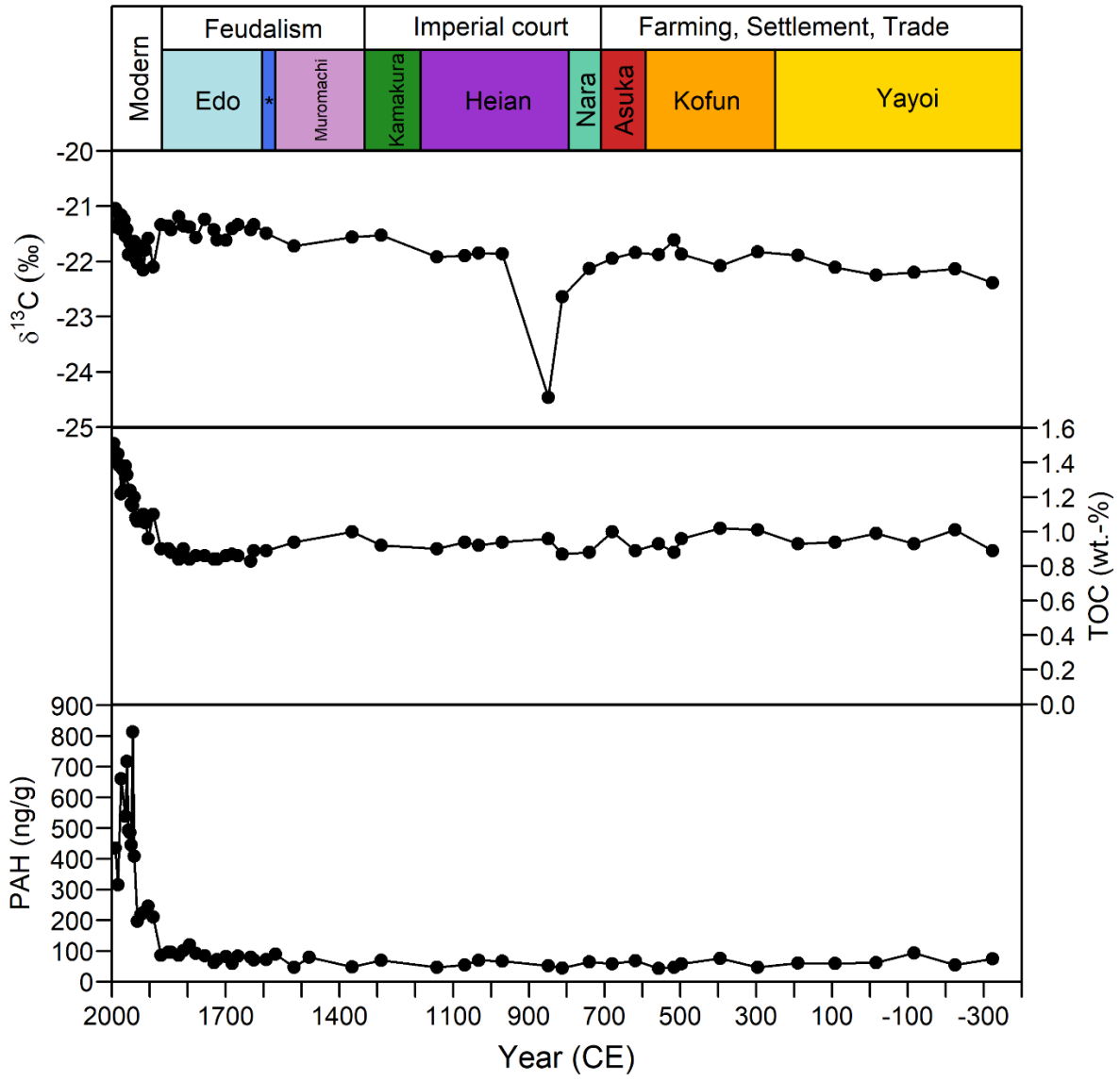

240

241 Figure 3. Temporal trend of $\delta^{13}C$ values, total organic carbon (TOC), and the sum of
242 polycyclic aromatic hydrocarbons (PAH) against total dry sample. *Azuchi-Momoyama
243 period.

244

Polycyclic aromatic hydrocarbons

The low-weight three-ring PAHs naphthalene, acenaphthylene, acenaphthene, and fluorene were often below the detection limit. Thus, the sum of PAHs (ΣPAH) in this study involved the following 12 PAHs: phenanthrene (Phe), anthracene (Ant), fluoranthene (Flt), pyrene (Pyr), benz[a]anthracene (BaA), chrysene (Chr), benzo[b]fluoranthene (BbF), benzo[k]fluoranthene (BkF), benzo[a]pyrene (BaP), benzo[g,h,i]perylene (BghiP), dibenz[a,h]anthracene (DahA), and indeno[1,2,3-cd]pyrene (IcdP). Overall, the ΣPAH concentrations ranged from about 40 to 800 ng g^{-1} throughout the core (Fig. 3). From the Yayoi to the end of the Azuchi-Momoyama period, between 320 BCE and 1603 CE, the ΣPAH concentration ranged between 43 and 91 ng g^{-1} without a clear pattern. The ΣPAH concentration started to increase from the early 1700s CE to about 1800 CE. Since then, it remained constant until about 1870 CE (Fig. 4). From then, the ΣPAH concentration increased until the early 1900s CE and remained constant again until the early 1930 CE. The peak in the ΣPAH concentration was observed at around 1945 CE and started to scatter towards the surface.

With respect to individual PAHs, Phe showed a relatively large scatter throughout the core (Fig. S3). Anthracene, Flt, and Pyr tended to increase towards the surface from the 1870s CE, and BaA and Chr increased from the early 18th century CE. Higher mass PAHs (> 228 g mol^{-1}) started to increase from the early 17th century CE.

The ratio of Flt/(Flt+Pyr) was relatively stable throughout the core (~0.60) until the end of the 17th century. Since then, a slight decrease to ~0.5 until the 20th century was observed (Fig. 5). Similarly, the ratio of LMW/total was relatively constant (~0.75) until the beginning of the 17th century CE and decreased to ~0.4 until the top of the core (Fig. 5). The

268 IcdP/(IcdP+BghiP) ratio was around 0.71 until the beginning of the 17th century CE and
269 decreased to approximately 0.5 towards the surface.

270 We found the logarithm of the ∑PAH concentration was positively correlated with the
271 logarithm of the Zn, Cu, and Pb concentrations (Fig. 6) determined in our previous study
272 (Nitzsche et al., 2022).

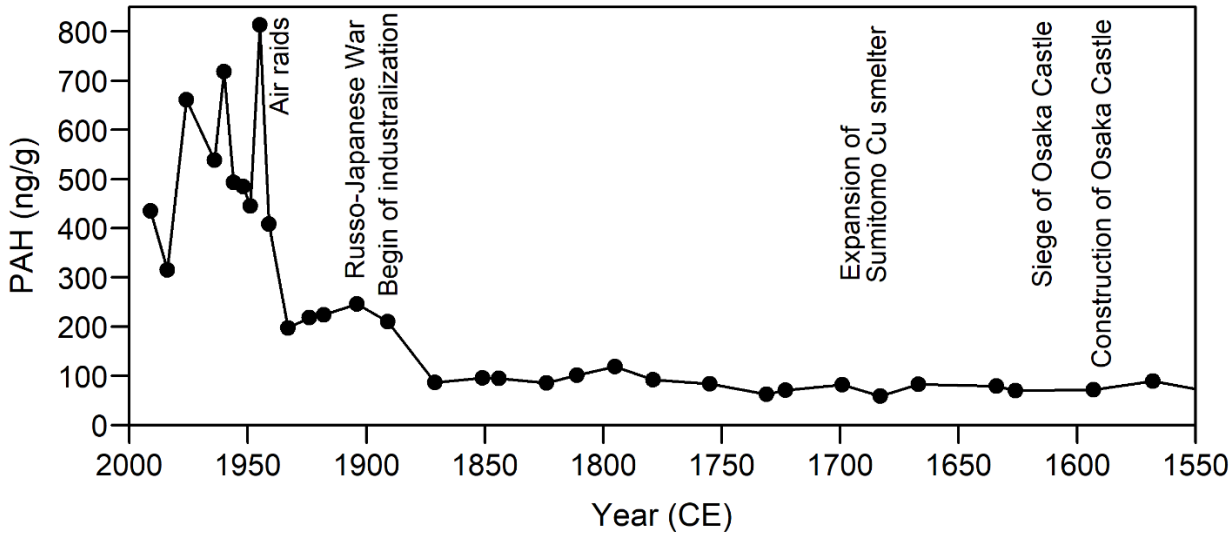

273

274 Figure 4. Temporal trend of the sum of polycyclic aromatic hydrocarbons (PAH) from 1550
275 to 2000 CE with major historical events in the catchment or Japan.

276

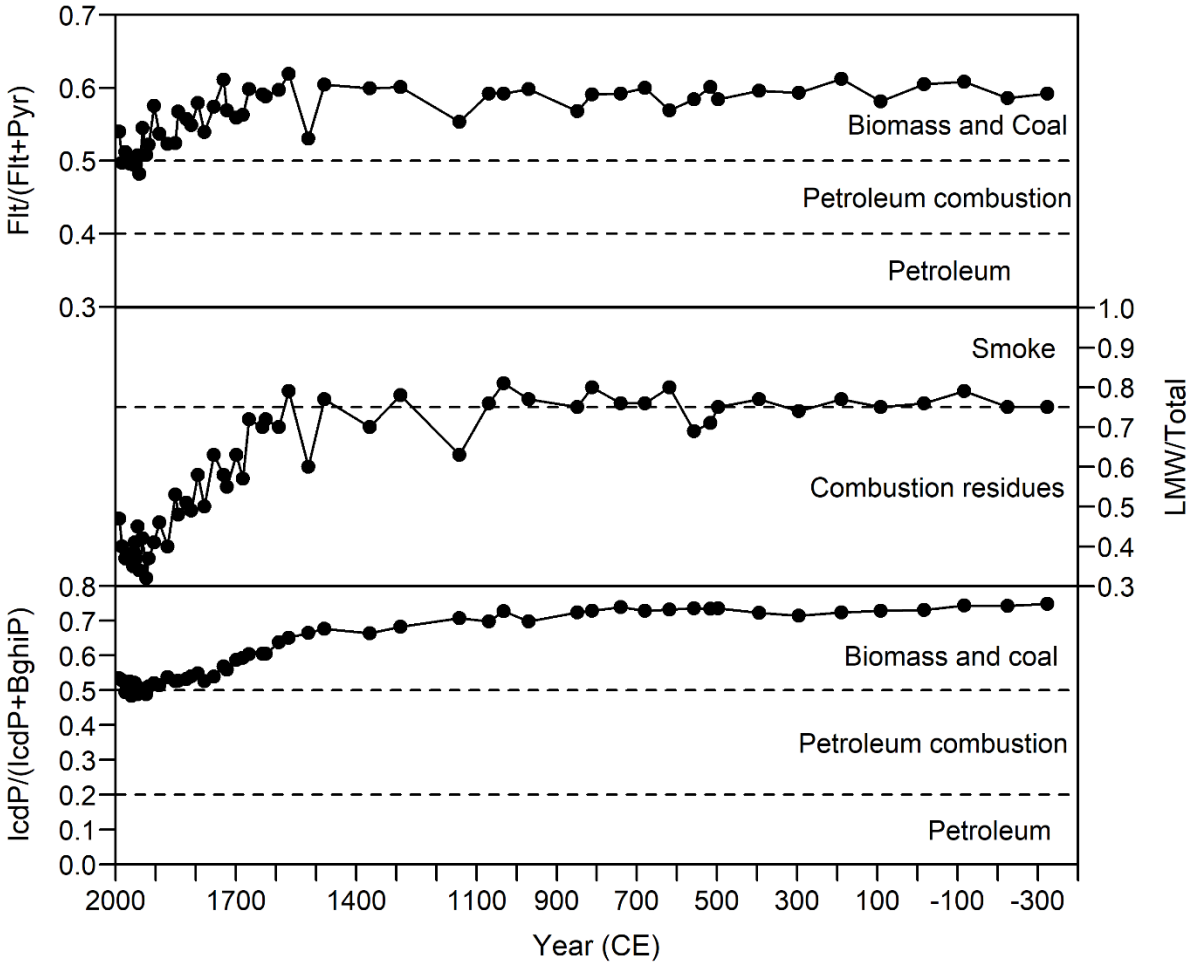

277

278 Figure 5. Historical trend of the ratios Flt/(Flt+Pyr), LMW/total, and IcdP/(IcdP+BghiP).

279

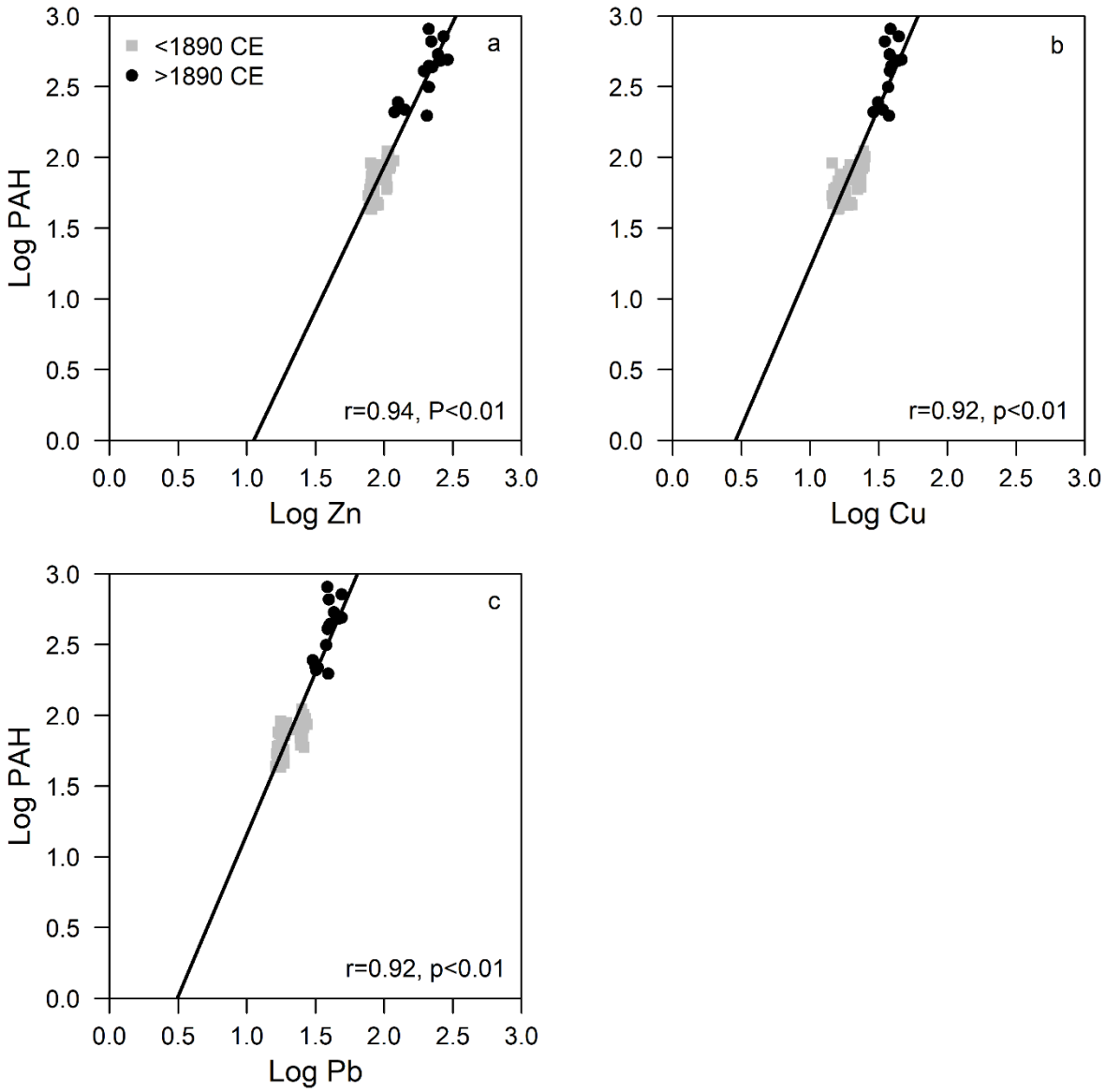

Figure 6. Scatterplot of the logarithm of the sum of polycyclic aromatic hydrocarbons (PAHs) against the logarithm of zinc (a), against the logarithm of copper (b), and against the logarithm of lead (c). The original Zn, Cu and Pb concentrations are reported in Nitzsche et al. (2022).

Discussion

Historical trend of PAHs before the Edo period

Based on the temporal changes in the ΣPAH concentration and composition, we gain insights into human activities in the catchment of Osaka Bay throughout time. Nevertheless,

290 the low ΣPAH concentration of < 100 ng and the lack of pattern before the 17th century CE
291 (Fig. 3) could be partly attributed to diagenetic alteration (Wakeham et al., 1980). For
292 instance, the diagnostic ratios of Ant/(Ant+Phe) and BaA/(BaA+Chr) (Yunker et al., 2002),
293 indicate petroleum before the 19th CE (Fig. S4). Yan et al. (2005) attributed similar unrealistic
294 patterns of Ant/(Ant+Phe) and BaA/(BaA+Chr) found in a 200-year-old sediment core from
295 Central Park Lake, New York City, to the higher photolytic breakdown of Ant and BaA
296 relative to Phe and Chr. Nevertheless, Ant and BaA contribute less than 10 % to the ΣPAH
297 concentration. Furthermore, small changes in the MAR could have caused dilution effects,
298 which could not be seen due to the temporal resolution of the core. The pattern of the ΣPAH
299 concentration from the beginning of the 17th century CE agreed to historical events.
300 Therefore, we consider diagenetic alteration to be minimal across the core. The increasing
301 concentration of perylene with increasing core depth (Fig. S5) agrees with previous studies,
302 which suggest a contribution of in-situ production of perylene by microbial communities
303 under anoxic conditions to the sediments (Gschwend and Hites, 1981; Silliman et al., 2001;
304 Slater et al., 2013). Furthermore, some perylene could have been derived from terrestrial
305 fungi (Grice et al., 2009; Itoh and Hanari, 2010).
306 The LMW/total ratios around 0.75 indicate that PAHs were derived from smoke rather
307 than combustion residues before the Edo period (Fig. 5) (Karp et al., 2020). Such PAHs likely
308 represent the deposition of natural PAHs derived from wildfires as well as anthropogenic
309 PAHs derived from softwood and charcoal combustion. Recent work has tested the source
310 area (up to 150 km) of PAHs originating from wildfires (Vachula et al., 2020). Yet, it is
311 difficult for the current dataset to estimate the exact source area because PAHs could have
312 additional origins than the Osaka Bay catchment owing to their potential for long-range
313 atmospheric transport (Halsall et al., 2001). For instance, PAHs could have originated from
314 wildfires in other areas of Japan, in China, the Korean peninsula and even Eastern Russia,

315 which are common sources of PAHs in western Japan today (Inomata et al., 2012, 2013; Tang
316 et al., 2002; Yang et al., 2007). Thus, the scatter in the ΣPAH concentration during the pre-
317 Edo times is difficult to explain. It should be noted that we did not find any change in the
318 trace metal concentrations before the Edo period (Nitzsche et al., 2022).
319 Interestingly, the warring activities during the Azuchi-Momoyama period (1568 to
320 1600 CE), such as the siege of the Ishiyama Hongan-ji temple (1569 to 1580 CE), were not
321 reflected in the ΣPAH concentration. While these events likely emitted PAHs to the
322 atmosphere via the combustion of wood and charcoal for weapon and armor smelting and the
323 burning of military and civil wooden buildings, tracing their impacts on the sedimentary Σ
324 PAH concentration would require a higher temporal revolution and/or the PAH emission
325 might be too low to be detected.
326
327 *Historical trend of PAHs during the Edo period*
328 Human impacts on the PAH concentration and composition are more apparent during
329 the Edo period. Since the Osaka Castle was destroyed by the Tokugawa forces in 1615 CE,
330 the local population and economy have continuously grown during the peaceful Edo period
331 which made Osaka City an important center for trade, culture, and food products. The
332 increasing ΣPAH concentration from the early 18th century CE until approximately 1800 CE
333 (Fig. 4) agree with the increasing population in the Osaka area from the mid-17th century CE
334 until the end of the 18th century CE (Saito, 2002). The LMW/total ratio decrease from the
335 beginning of the 17th century CE (Fig. 5) indicates a shift from smoke to particulate PAHs.
336 Combustion residues from biomass and charcoal could have directly entered the rivers and
337 seawater and finally deposited in the sediment. During the Edo period, charcoal gained a
338 widespread importance, and a new type of white charcoal, the so-called *binchotan*, was

combusted after being transported from Wakayama Prefecture (Totman and Kumazaki, 1998). Another PAH source could be the start of salt production in the Seto Inland Sea area, which required the burning of large amounts of wood and charcoal leading to barren areas in the mountains.

The increasing ΣPAH concentration from the early 18th century CE until approximately 1800 CE is consistent with an increase in the Cu concentration observed in the same core until the beginning of the 19th century CE (Nitzsche et al., 2022). This was attributed to emissions from ore smelting by the Sumitomo Copper Refinery, established 1 km southwest of Osaka Castle in 1655 CE and expanded in 1690 CE (Suzuki et al., 1998). Thus, the burning of wood and charcoal for heat and energy generation and the early usage of oil lamps are likely sources of human-derived PAHs. The constant ΣPAH concentration until the late 19th century overlaps with a decline in population in the Osaka area, which started at the end of the 18th century CE (Saito, 2002). The big city fires in 1724, 1837, and 1863 CE could not be detected in the core which requires a higher temporal resolution and/or the PAH emissions were too low to be detected.

Historical trend of PAHs during the Modern age

The rapid tripling of the ΣPAH concentration from the end of the 19th century CE until the beginning of the 20th century CE is associated with increasing Cu, Zn, and Pb concentrations in the core and marked the beginning of industrialization (Nitzsche et al., 2022). The further decreasing LMW/total ratio from the 1870s CE could be due to the combustion of imported and mined coal. The development of the iron and steel industry, Cu smelters, shipbuilding, and other industries, as well as steam ships, emitted large amounts of smoke into the atmosphere and combustion residues into the rivers and the bay. Furthermore, Japan participated in the Shino-Japanese War (1894-1895), the Russo-Japanese War

(1904/1905) and World War I (1914 to 1918 CE). An increase in the ΣPAH concentration was also observed in a core from Osaka Castle moat, yet about 25 years earlier (Moriwaki et al., 2005), which could be due to uncertainties in age models, differences in the time of deposition as well as local impacts in the vicinity of Osaka Castle. The relatively constant ΣPAH concentration from the mid-1910s CE until the early 1930s CE could partly be explained by a relatively stagnant economy in Japan (1929 to 1932 CE). A relatively constant ΣPAH concentration was also observed between the early 1900s and the early 1920s CE in a core from Tokyo Bay (Yamashita et al., 2000). The peak in the ΣPAH concentration around 1945 CE was also observed in the Osaka Castle moat (Moriwaki et al., 2005) and Nagaike Pond, a reservoir in the South of Osaka City (Ishitake et al., 2007), which was explained by burning of wooden buildings due to the heavy bombing raids on Osaka and Kobe City during World War II. In addition, traffic-related PAHs became an important source after World War II. A high ΣPAH concentration during the late 1970s CE was also detected in a coastal core close to the Yodo River mouth and marked the beginning of the use of cleaner energy and coal filters during the 1980s (Tsuji et al., 2020). The diagnostic Flt/(Flt+Pyr) and IcdP/(IcdP+BghiP) ratios suggest biomass, coal, and petroleum combustion during the 20th century CE (Fig. 5), which agrees with surface sediments in Osaka Bay (Tsuji et al., 2020). Thus, the transition from coal to oil around 1950 CE is not clearly observed in the core.

Contemporaneous changes in the ΣPAH and trace metal, in particular Pb, concentrations in sediment cores are often observed and explained by similar elemental sources such as smelting (Azoury et al., 2013; Leorri et al., 2014; Musa Bandowe et al., 2014; Wang et al., 2018). In the case of Osaka Bay, the contemporaneous increase in ΣPAH and Cu, Zn, Pb concentrations from the late 19th century CE (Nitzsche et al., 2022) and peak

around 1960 CE is confirmed by positive correlations between the ΣPAH with Cu, Zn and Pb concentrations in the sediment core (Fig. 6). The results indicate the combustion of wood and charcoal during the 18th and 19th centuries and of coal from the late 19th century CE for smelting and other industrial activities. The introduction of ash filters and transition from coal to oil could have led to a decline in ΣPAH and trace metal concentrations from the early 1960s CE. In the case of trace metals, the decline was also promoted by the regulation of sewage waters and industrial effluents. More insights into the shared PAH and Pb sources can be gained by Pb stable isotopes (Leorri et al., 2014).

Summary and conclusions

This study successfully compared the PAH record in a coastal marine sediment core with historical events and human activities. The total PAH concentration and LMW/total ratio before the beginning of the 17th century CE were relatively constant and mainly reflected smoke-derived PAHs from the natural background. A shift to a higher relative abundance of concentrations of 4−6 ring PAHs from the early 17th century CE and a higher PAH concentration from the early 18th century CE until approximately 1800 CE agreed with a population increase and increasing importance of charcoal during the peaceful Edo period. The constant PAH concentration until the late 19th century CE overlapped with a decline in the local population, while the increasing PAH concentration from the late 19th century CE marks the beginning of industrialization. The peak in PAH concentration in 1945 CE was caused by burning of the wooden structures due to air raids on Osaka City.

The combination of PAHs with trace metals, in particular Cu and Pb, yielded insights into related sources, i.e., combustion of wood and charcoal (PAH source) for smelting Cu ores (Cu source) during the 18th century CE, and combustion of coal for smelting and heavy industries from the end of the 19th century CE. Our results demonstrate that PAH concentrations and

412 diagnostic ratios in coastal sediment cores can be used to reconstruct pre-industrial human
413 activities.
414
415 **Acknowledgements**
416 We thank Ami Togami (AORI), Yosuke Miyairi (AORI), Masafumi Murayama (Kochi Core
417 Center), Hiroyuki Matsuzaki (MALT), and the onboard scientists of the KT-11-13 cruise for
418 their support in core drilling, slicing, grain size and radiocarbon analysis. We kindly thank the
419 anonymous reviewer and the editor for their constructive comments, which greatly helped to
420 improve this manuscript.
421
422 **Funding**
423 K. N. Nitzsche was supported by the JAMSTEC Young Research Fellowship.
424
425 **References**
426 Allen JRL (2000) Morphodynamics of Holocene salt marshes: A review sketch from the
427 Atlantic and Southern North sea coasts of Europe. *Quaternary Science Reviews* 19(17–
428 18): 1839–1840.
429 Argiriadis E, Battistel D, McWethy DB, et al. (2018) Lake sediment fecal and biomass
430 burning biomarkers provide direct evidence for prehistoric human-lit fires in New
431 Zealand. *Scientific Reports* 8(1): 2–10.
432 Azoury S, Troncynski J, CHiffoleau J-F, et al. (2013) Historical Records of Mercury, Lead,
433 and Polycyclic Aromatic Hydrocarbons Depositions in a Dated Sediment Core from the
434 Eastern Mediterranean. *Environmental Science and Technology* 47(13): 7101–7109.
435 Baek SO, Field RA, Goldstone ME, et al. (1991) A review of atmospheric polycyclic
436 aromatic hydrocarbons: Sources, fate and behavior. *Water, Air, and Soil Pollution* 60:
437 279–300.

438 Barletta M, Lima ARA and Costa MF (2019) Distribution, sources and consequences of
439 nutrients, persistent organic pollutants, metals and microplastics in South American
440 estuaries. *Science of the Total Environment* 651: 1199–1218.
441 Bronk Ramsey C (2009) Bayesian analysis of radiocarbon dates. *Radiocarbon* 51(1): 337–
442 360.
443 de Souza Machado AA, Spencer K, Kloas W, et al. (2016) Metal fate and effects in estuaries:
444 A review and conceptual model for better understanding of toxicity. *Science of the Total*
445 *Environment* 541: 268–281.
446 Elmquist M, Zencak Z and Gustafsson Ö (2007) A 700 year sediment record of black carbon
447 and polycyclic aromatic hydrocarbons near the EMEP air monitoring station in
448 Aspvreten, Sweden. *Environmental Science and Technology* 41(20): 6926–6932.
449 Grice K, Lu H, Atahan P, et al. (2009) New insights into the origin of perylene in geological
450 samples. *Geochimica et Cosmochimica Acta* 73(21): 6531–6543.
451 Gschwend PM and Hites RA (1981) Fluxes of polycyclic aromatic hydrocarbons to marine
452 and lacustrine sediments in the northeastern United States. *Geochimica et Cosmochimica*
453 *Acta* 45(12): 2359–2367.
454 Guo W, Luo X, Hou G, et al. (2023) A century-long record of polycyclic aromatic
455 hydrocarbon deposition in the Old Yellow River Estuary, China. *Marine Pollution*
456 *Bulletin* 196: 115643.
457 Halsall CJ, Sweetman AJ, Barrie LA, et al. (2001) Modelling the behaviour of PAHs during
458 atmospheric transport from the UK to the Arctic. *Atmospheric Environment* 35(2): 255–
459 267.
460 Heaton TJ, Köhler P, Butzin M, et al. (2020) Marine20 - The marine radiocarbon age
461 calibration curve (0-55,000 cal BP). *Radiocarbon* 62(4): 779–820.
462 Hosono T, Su C-C, Okamura K, et al. (2010) Historical record of heavy metal pollution
463 deduced by lead isotope ratios in core sediments from the Osaka Bay, Japan. *Journal of*

464 *Geochemical Exploration* 107(1): 1–8.
465 Inomata Y, Kajino M, Sato K, et al. (2012) Emission and atmospheric transport of particulate
466 PAHs in Northeast Asia. *Environmental Science and Technology* 46(9): 4941–4949.
467 Inomata Y, Kajino M, Sato K, et al. (2013) Source contribution analysis of surface particulate
468 polycyclic aromatic hydrocarbon concentrations in northeastern Asia by source-receptor
469 relationships. *Environmental Pollution* 182: 324–334.
470 Ishitake M, Moriwaki H, Katahira K, et al. (2007) Vertical profile of polycyclic aromatic
471 hydrocarbons in a sediment core from a reservoir in Osaka City. *Environmental Geology*
472 52(1): 123–129.
473 Islam MS and Tanaka M (2004) Impacts of pollution on coastal and marine ecosystems
474 including coastal and marine fisheries and approach for management: A review and
475 synthesis. *Marine Pollution Bulletin* 48(7–8): 624–649.
476 Itihara M, Yoshikawa S, Kamei T, et al. (1988) Stratigraphic Subdivision of Quaternary
477 Deposits in Kinki District, Japan. *Memoirs of the Geological Society of Japan* 30: 111–
478 125 (In Japanese).
479 Itoh N and Hanari N (2010) Possible precursor of perylene in sediments of Lake Biwa
480 elucidated by stable carbon isotope composition. *Geochemical Journal* 44: 161–166.
481 Kajita H, Kawahata H, Wang K, et al. (2018) Extraordinary cold episodes during the mid-
482 Holocene in the Yangtze delta: Interruption of the earliest rice cultivating civilization.
483 *Quaternary Science Reviews* 201: 418–428.
484 Kajita H, Isaji Y, Kato R, et al. (2023) Climatic change around the 4.2 ka event in coastal
485 areas of the East China Sea and its potential influence on prehistoric Japanese people.
486 *Paleogeography, Paleoclimatology, Paleoecology* 609: 111310.
487 Kajiyama H and Itihara M (1972) The developmental history of the Osaka Plain with
488 references to the radio-carbon dates. *The Geological Society of Japan* 7: 101–112 (In
489 Japanese).

490 Karp AT, Holman AI, Hopper P, et al. (2020) Fire distinguishers: Refined interpretations of
491 polycyclic aromatic hydrocarbons for paleo-applications. *Geochimica et Cosmochimica*
492 *Acta* 289: 93–113.
493 Kawahata H, Matsuoka M, Togami A, et al. (2017) Climatic change and its influence on
494 human society in western Japan during the Holocene. *Quaternary International* 440:
495 102–117.
496 Kuo LJ, Louchouarn P, Herbert BE, et al. (2011) Combustion-derived substances in deep
497 basins of Puget Sound: Historical inputs from fossil fuel and biomass combustion.
498 *Environmental Pollution* 159(4): 983–990.
499 Kuwae M, Yamamoto M, Ikehara K, et al. (2013) Stratigraphy and wiggle-matching-based
500 age-depth model of late Holocene marine sediments in Beppu Bay, southwest Japan.
501 *Journal of Asian Earth Sciences* 69: 133–148.
502 Lazzari L, Wagener ALR, Boyle EA, et al. (2019) Sedimentary record of hydrocarbons and
503 sewage inputs from a highly populated region in South-Eastern Brazil. *Marine Pollution*
504 *Bulletin* 149: 110565.
505 Leorri E, Mitra S, Irabien MJ, et al. (2014) A 700year record of combustion-derived pollution
506 in northern Spain: Tools to identify the Holocene/Anthropocene transition in coastal
507 environments. *Science of the Total Environment* 470–471: 240–247.
508 Liu GQ, Zhang G, Li XD, et al. (2005) Sedimentary record of polycyclic aromatic
509 hydrocarbons in a sediment core from the Pearl River Estuary, South China. *Marine*
510 *Pollution Bulletin* 51(8–12): 912–921.
511 Lotze HK, Lenihan HS, Bourque BJ, et al. (2006) Depletion, Degradation, and Recovery
512 Potential of Estuaries and Coastal Seas. *Science* 312(5781): 1806–1809.
513 Matsuda J (2008) New perspectives in archaeology: Earth science at the archaeological sites
514 (4) For reconstruction of landscape. *Quarterly of Archaeological Studies* 54: 108–111 (In
515 Japanese).

516 Matsuzaki H, Nakano C, Yamashita H, et al. (2004) Current status and future direction of
517 MALT, The University of Tokyo. *Nuclear Instruments and Methods in Physics Research*
518 *Section B: Beam Interactions with Materials and Atoms* 223–224: 92–99.
519 Moriwaki H, Katahira K, Yamamoto O, et al. (2005) Historical trends of polycyclic aromatic
520 hydrocarbons in the reservoir sediment core at Osaka. *Atmospheric Environment* 39(6):
521 1019–1025.
522 Musa Bandowe BA, Srinivasan P, Seelge M, et al. (2014) A 2600-year record of past
523 polycyclic aromatic hydrocarbons (PAHs) deposition at Holzmaar (Eifel, Germany).
524 *Palaeogeography, Palaeoclimatology, Palaeoecology* 401: 111–121.
525 Nitzsche KN, Yoshimura T, Ishikawa NF, et al. (2022) Metal contamination in a sediment
526 core from Osaka Bay during the last 400 years. *Progress in Earth and Planetary Science*
527 9: 58.
528 Ogawa NO, Nagata T, Kitazato H, et al. (2010) Ultra-sensitive elemental analyzer/isotope
529 ratio mass spectrometer for stable nitrogen and carbon isotope analyses. In: Ohkouchi N,
530 Tayasu I, and Koba K (eds) *Earth, Life, and Isotopes*. Kyoto University Press, pp. 339–
531 353.
532 Pearson R (2016) *Ōsaka Archaeology*. Oxford: Archaeopress Publishing Ltd.
533 Reeder-Myers L, Braje TJ, Hofman CA, et al. (2022) Indigenous oyster fisheries persisted for
534 millennia and should inform future management. *Nature Communications* 13(1): 2383.
535 Saito O (2002) *Edo and Osaka: An Origin of Modern Japanese Cities*. Tokyo: NTT
536 Publishing (In Japanese).
537 Silliman JE, Meyers PA, Eadie BJ, et al. (2001) A hypothesis for the origin of perylene based
538 on its low abundance in sediments of Green Bay, Wisconsin. *Chemical Geology* 177(3–
539 4): 309–322.
540 Slater GF, Benson AA, Marvin C, et al. (2013) PAH fluxes to Siskiwit revisted: Trends in
541 fluxes and sources of pyrogenic PAH and perylene constrained via radiocarbon analysis.

Environmental Science and Technology 47(10): 5066–5073.

Sun X, Li C, Kuiper KF, et al. (2016) Human impact on erosion patterns and sediment transport in the Yangtze River. *Global and Planetary Change* 143: 88–99.

Sun Y, Ogawa NO, Ishikawa NF, et al. (2023) Application of a porous graphitic carbon column to carbon and nitrogen isotope analysis of underivatized individual amino acids using high-performance liquid chromatography coupled with elemental analyzer/isotope ratio mass spectrometry. *Rapid Communications in Mass Spectrometry* 37(17): 1–10.

Suzuki H, Matsuo N, Ito K, et al. (1998) *Archaeological Reports of the Sumitomo Copper Refinery Site* (OCCP Associationed.). Osaka: Osaka City Cultural Properties Association (In Japanese).

Tang N, Tabata M, Mishukov VF, et al. (2002) Comparison of atmospheric nitropolycyclic aromatic hydrocarbons in Vladivostok, Kanazawa and Toyama. *Journal of Health Science* 48(1): 30–36.

Tayasu I, Hirasawa R, Ogawa NO, et al. (2011) New organic reference materials for carbon- and nitrogen-stable isotope ratio measurements provided by Center for Ecological Research, Kyoto University, and Institute of Biogeosciences, Japan Agency for Marine-Earth Science and Technology. *Limnology* 12(3): 261–266.

Tobiszewski M and Namieśnik J (2012) PAH diagnostic ratios for the identification of pollution emission sources. *Environmental Pollution* 162: 110–119.

Topness RG, Vachula RS, Balascio NL, et al. (2023) Northern Norway paleofire records reveal two distinct phases of early human impacts on fire activity. *Holocene* 33(11): 1304–1316.

Totman C and Kumazaki M (1998) *The Green Archipelago: Forestry in Pre-Industrial Japan (Nihonjin Ha Donoyoni Mori Wo Tsukuttekitanoka)*. Tokyo: Tsukiji Shokan Publishing (In Japanese).

Tsuji H, Jadoon WA, Nunome Y, et al. (2020) Distribution and source estimation of

568 polycyclic aromatic hydrocarbons in coastal sediments from Seto Inland Sea, Japan.
569 *Environmental Chemistry* 17(7): 488–497.
570 Vachula RS, Huang Y, Russell JM, et al. (2020) Sedimentary biomarkers reaffirm human
571 impacts on northern Beringian ecosystems during the Last Glacial period. *Boreas* 49(3):
572 514–525.
573 Vachula RS, Karp AT, Denis EH, et al. (2022) Spatially calibrating polycyclic aromatic
574 hydrocarbons (PAHs) as proxies of area burned by vegetation fires: Insights from
575 comparisons of historical data and sedimentary PAH fluxes. *Palaeogeography,*
576 *Palaeoclimatology, Palaeoecology* 596: 110995.
577 Wakeham S, Schaffner C and Giger W (1980) Polycyclic aromatic hydrocarbons in Recent
578 lake sediments — II . Compounds derived from biogenic precursors during early
579 diagenesis. *Geochimica et Cosmochimica Acta* 44: 415–429.
580 Wang L, Chen G, Kang W, et al. (2018) Sediment evidence of industrial leakage-induced
581 asynchronous changes in polycyclic aromatic hydrocarbons and trace metals from a sub-
582 trophic lake, southwest China. *Environmental Science and Pollution Research* 25:
583 13035–13047.
584 Wang Z, Fingas M and Page DS (1999) Oil spill identification. *Journal of Chromatography A*
585 843: 369–411.
586 Wilcke W (2007) Global patterns of polycyclic aromatic hydrocarbons (PAHs) in soil.
587 *Geoderma* 141(3–4): 157–166.
588 Yamashita N, Kannan K, Imagawa T, et al. (2000) Vertical profile of polychlorinated
589 dibenzo-p-dioxins, dibenzofurans, naphthalenes, biphenyls, polycyclic aromatic
590 hydrocarbons, and alkylphenols in a sediment core from Tokyo Bay, Japan.
591 *Environmental Science and Technology* 34(17): 3560–3567.
592 Yan B, Abrajano TA, Bopp RF, et al. (2005) Molecular tracers of saturated and polycyclic
593 aromatic hydrocarbon inputs into Central Park Lake, New York City. *Environmental*

Science and Technology 39(18): 7012–7019.

Yan B, Abrajano TA, Bopp RF, et al. (2006) Combined application of δ13C and molecular ratios in sediment cores for PAH source apportionment in the New York/New Jersey harbor complex. *Organic Geochemistry* 37(6): 674–687.

Yang XY, Okada Y, Tang N, et al. (2007) Long-range transport of polycyclic aromatic hydrocarbons from China to Japan. *Atmospheric Environment* 41(13): 2710–2718.

Yasuhara M and Yamazaki H (2005) The impact of 150 years of anthropogenic pollution on the shallow marine ostracode fauna, Osaka Bay, Japan. *Marine Micropaleontology* 55(1–2): 63–74.

Yasuhara M, Irizuki T, Yoshikawa S, et al. (2002) Holocene sea-level changes in Osaka Bay, western Japan: ostracode evidence in a drilling core from the southern Osaka Plain. *The Journal of the Geological Society of Japan* 108(10): 633–643.

Yokoyama Y, Miyairi Y, Matsuzaki H, et al. (2007) Relation between acid dissolution time in the vacuum test tube and time required for graphitization for AMS target preparation. *Nuclear Instruments and Methods in Physics Research Section B* 259(1): 330–334.

Yokoyama Y, Miyairi Y, Aze T, et al. (2019) A single stage Accelerator Mass Spectrometry at the Atmosphere and Ocean Research Institute, The University of Tokyo. *Nuclear Instruments and Methods in Physics Research Section B: Beam Interactions with Materials and Atoms* 456(15): 311–316.

Yoon SJ, Hong S, Lee Junghyun, et al. (2023) Historical trends of traditional, emerging, and halogenated polycyclic aromatic hydrocarbons recorded in core sediments from the coastal areas of the Yellow and Bohai seas. *Environment International* 178: 108037.

Yunker MB, Macdonald RW, Vingarzan R, et al. (2002) PAHs in the Fraser River basin: a critical appraisal of PAH ratios as indicators of PAH source and composition. *Organic Geochemistry* 33: 489–515.

Zong Y, Yu F, Huang G, et al. (2010) Sedimentary evidence of Late Holocene human activity

in the Pearl River delta, China. *Earth Surface Processes and Landforms* 35(9): 1095–1102.

Supplementary information